Weyl's relations, integrable matrix models, and quantum computation

B. Sriram Shastry [*]
Physics Department, University of California, Santa Cruz, California 95064, USA

Emil A. Yuzbashyan [†]
Department of Physics and Astronomy, Center for Materials Theory, Rutgers University, Piscataway, New Jersey 08854, USA

Aniket Patra [‡]
Center for Theoretical Physics of Complex Systems, Institute for Basic Science, Daejeon 34126, Republic of Korea

(Received 21 October 2025; accepted 12 February 2026; published 13 March 2026)

Starting from a generalization of Weyl's relations in finite dimension N, we show that the Heisenberg commutation relations can be satisfied in a specific $(N-1)$-dimensional subspace and display a linear map for projecting operators to this subspace. This setup is used to construct a hierarchy of parameter-dependent commuting matrices in N dimensions. This family of commuting matrices is then related to type-1 matrices representing quantum integrable models. The commuting matrices find an interesting application in quantum computation, specifically in Grover's database search problem. Each member of the hierarchy serves as a candidate Hamiltonian for quantum adiabatic evolution and, in some cases, achieves higher fidelity than standard choices, thus offering improved performance.

DOI: 10.1103/vvky-3ghn

I. INTRODUCTION

In this work, we present a link between Weyl's relations, commuting matrices, and quantum computation within the context of finite-dimensional matrices representing quantum systems in finite-dimensional Hilbert spaces. To this end, we construct a class of mutually commuting real symmetric $N \times N$ matrices that depend linearly on a parameter x, representing quantum integrable systems in finite dimensions. They are obtained from algebra involving three matrices $(\mathcal{E}, \mathcal{S}, \mathbf{\Gamma})$ in a structure that is closely related to generalizations of matrices appearing in Weyl's relations [1–4]. Weyl's concern was with the emergence of the Heisenberg commutation relations in the limit of large dimensions. We display variants of the Weyl matrices defining Weyl's relations in finite dimensions, which yield canonical commutators in well-defined subspaces defined by the orthogonality with respect to a single specific state. Using these commutators, we construct a hierarchy of commuting matrices and find that they coincide with certain linear combinations of type-1 commuting matrices previously obtained by us [5–11] using entirely different arguments.

We show that the commuting matrices found here generalize a model Hamiltonian studied in the context of quantum computation. It is used to display the quantum advantage over classical methods in the problem of a search in a random database, i.e., Grover's algorithm as implemented through adiabatic evolution [12–21].

A detailed review of type-1 matrices is given in [9]. They constitute a class of finite-dimensional matrices that aim to capture the essence of quantum integrability at the level of a matrix representation of models, rather than at the more conventional Hamiltonian level involving physical degrees of freedom. Here we derive the type-1 commuting matrices from the commutation relation (26).

We first discuss the Weyl relations in the large-N limit in Sec. II, where the Weyl matrices A and B [see Eqs. (5) and (3)] are introduced, and a review of how the Heisenberg algebra emerges from them is provided while taking a careful continuum limit [2,4,48]. In Sec. III, we summarize earlier generalizations of Weyl's operator basis of Eq. (11), which are used to create a basis of operators representing maximally entangled states. We then introduce a matrix C [Eq. (12)], a different generalization of the Weyl matrices, which together with B defines the algebra in Eq. (14), which plays an important role in the subsequent analysis. This is a simplified version of the algebra found in Sec. IV in Eq. (26), which is finally employed to generate the commuting matrices in Sec. V. In Sec. VI, we discuss the use of the type-1 matrices in implementing the Grover algorithm through adiabatic computation. By studying the fidelity, we show that the higher-order matrices lead to an increase in the efficiency of computation. In Sec. VII, we make some final remarks.

II. WEYL MATRICES AND THE LIMIT $N \to \infty$

Weyl proposed an important pathway for understanding the Heisenberg algebra

$$[Q, P] = i\hbar \mathbb{1}, \tag{1}$$

[*]Contact author: sriram@physics.ucsc.edu
[†]Contact author: eyuzbash@physics.rutgers.edu
[‡]Contact author: patraaniket@gmail.com

 ©2026 American Physical Society

which emerges from a finite-dimensional setting in the limit of infinite dimensions. Taking the limit of infinite dimensions is necessary to avoid a familiar contradiction arrived at by taking the trace of the Heisenberg algebra in finite dimensions. Weyl's work was followed by others detailing and extending his arguments [1–4]. Since our work relies on yet another extension of Weyl's work, before describing it we first provide a quick summary of the known results.

Weyl began with a relation for a pair of $N \times N$ unitary matrices A and B,

$$AB = BAe^{i\omega_0}, \tag{2}$$

where $\omega_0 = \frac{2\pi}{N}$ and $e^{i\omega_0}$ is the Nth root of unity with integer N, taken to infinity at the end. It follows from iteration that $A^N = \mathbb{1} = B^N$. The form of the matrices is determined as follows: First, we set B to be a diagonal with diagonal entries $\{b_0, b_1, \ldots, b_{N-1}\}$ and $b_r = e^{i\omega_0 r}$ (thus satisfying $B^N = \mathbb{1}$), i.e.,

$$B = \sum_{n=0}^{N-1} b_n |n\rangle\langle n|. \tag{3}$$

On taking the matrix elements of Eq. (2), we get (for $0 \leqslant \{i, j\} \leqslant N-1$) the conditions

$$A_{ij} b_j = e^{i\omega_0}\, b_i A_{ij}. \tag{4}$$

Together with the choice $b_n = e^{i\omega_0 n}$, this implies that the only nonzero elements of A are of the form $A_{j,j+1}$, and we may represent A as

$$A = \sum_{n=0}^{N-1} |n-1\rangle\langle n|, \tag{5}$$

with periodic boundary conditions $n \equiv n + N$. Thus, A is the left-shift operator on a ring of sites of length N. A is diagonalized in the plane-wave basis

$$|k_r\rangle = \frac{1}{\sqrt{N}} \sum_{n=0}^{N-1} e^{ik_r n} |n\rangle, \tag{6}$$

where $k_r = r\,\omega_0$ and $0 \leqslant r \leqslant N-1$, so that $A|k_r\rangle = e^{ik_r}|k_r\rangle$, and

$$A = \sum_r e^{ik_r} |k_r\rangle\langle k_r|. \tag{7}$$

We first consider the limit of $N \to \infty$. Weyl showed that the Heisenberg algebra emerges from the Weyl relation (2) by expanding both sides for large N. This process requires a definition of the position operator $\hat{Q}$ and the momentum operator $\hat{P}$, which are defined by

$$A = e^{i\xi \hat{P}/\hbar}, \quad B = e^{i\eta \hat{Q}}, \tag{8}$$

together with the requirement that ξ and η are each of $O(\frac{1}{\sqrt{N}})$. With this, Eq. (2) vanishes to $O(\frac{1}{N^2})$, provided

$$\xi\eta\,[\hat{Q}, \hat{P}] = i\hbar\omega_0. \tag{9}$$

This leads to the Heisenberg algebra (1), provided

$$\xi\eta = \omega_0. \tag{10}$$

We discuss the details of this derivation in the Appendix.

III. WEYL MATRICES WITH FINITE N

Generalizations of Weyl's matrices A and B for finite N have recently received much interest in quantum computation. They are useful because they form a basis of N^2 operators representing maximally entangled states [22–24] and are referred to as the Weyl operator basis. Each element of the N^2-dimensional operator basis is explicitly given by

$$U_{n,m} = \sum_{r=0}^{N-1} e^{ink_r} |k_r\rangle\langle k_{r+m}|, \tag{11}$$

where n and m range over $0, N-1$. These matrices are extensions of the Weyl matrix A given in the form of (7).

We turn to a generalization of Weyl's operators in a different direction guided by the following question: Is it possible to preserve Eq. (1) as an operator identity while keeping the dimension N finite when acting on a well-defined subspace? One is faced with a similar question when quantizing constrained field theories, where the constraint is satisfied only as an operator acting on the physical states. This leads us to define another class of matrices in which the analog of Eq. (1) is satisfied on an $(N-1) \times (N-1)$ subspace of the original $N \times N$ space of states.

Towards this end, we now define a matrix operator C through the formula

$$C = \frac{1}{2} \sum_{n \neq m} \frac{|n\rangle\langle m| - |m\rangle\langle n|}{b_n - b_m}. \tag{12}$$

This matrix is closely related to $\ln A$ of Eq. (A7), with the omission of the b_m and b_n in the numerator of the second term. Note that C in Eq. (12) and B in Eq. (3) are defined in terms of b_n and the following property is independent of the choice of b_n. The commutator of C with B in Eq. (3) is computed as

$$[C, B] = \sum_{n \neq m} (|n\rangle\langle m|) \tag{13}$$

$$= \mathbb{1} - N|\psi\rangle\langle\psi|, \tag{14}$$

where the projection operator is constructed from the normalized "flat state" $|\psi\rangle$, which is defined as

$$|\psi\rangle = \frac{1}{\sqrt{N}} \sum_n |n\rangle = |k_{r=0}\rangle \tag{15}$$

and is also the zero wave-vector ($k_r = 0$) state from Eq. (6). From Eq. (14), we see that

$$[C, B]\,|\Psi\rangle = |\Psi\rangle \tag{16}$$

for any state $|\Psi\rangle = \sum_{r\neq 0} \alpha_r |k_r\rangle$ for arbitrary α_r. This implies that Eq. (16) remains valid as long as $|\Psi\rangle$ is contained in the $(N-1)$-dimensional subspace spanned by the basis $|k_r\rangle$ with $r \neq 0$, i.e., the subspace orthogonal to the state $|k_{r=0}\rangle$. The trace of $[C, B]$ vanishes due to the contribution from the last term. In this sense, the conjugate $N \times N$ matrices C and B come close to the canonical infinite-dimensional Heisenberg algebra (1). A particular advantage of the structure of C is that the commutator (14) is valid for an arbitrary choice of b_n, including real values. Below, we show the close connection of B and C to matrices that arise in the context of the type-1 integrable family, with both using real values for b_n.

We note that the matrix C can be written in the k representation by using Eq. (6) as

$$C = \frac{N}{2\pi}\sum_{r=0}^{N-1} k_r |k_r\rangle\langle k_{r+1}|, \tag{17}$$

which is a minimally off-diagonal version of the log-Weyl matrix $\ln A$ from Eq. (A8). The algebra satisfied by C seems to be quite rich. We quote one further result found by commuting the expressions in Eq. (A6) with the one in Eq. (17):

$$[\ln A, C] = -iC. \tag{18}$$

This result is reminiscent of the Fock commutator of $[p, \frac{1}{2}(px + xp)] = -i\hbar$, which is used to obtain the virial theorem in quantum theory. The commutator $[\ln B, C]$ is not related simply to C, so the analogy is only partial. We also note that matrix C in Eq. (17) is similar to matrix U_{11} in Eq. (11) and is obtained, up to an overall prefactor, when e^{ik_r} is replaced by ik_r.

In summary, the three matrices [C in Eq. (12) and A and B in Eq. (2)] and their logarithms introduced in Eqs. (A7) and (A5) satisfy the basic commutation results (14) and (18) for the special choice of $b_n = e^{i\omega_0 n}$. These relations, with the exception of Eq. (18), generalize to arbitrary choices of b_n. We may qualitatively view B as the position variable itself, and then A can be viewed as the discrete translation operator. The role of C is somewhat context driven. In Eq. (18) C is analogous to the Fock operator $xp + px$, but in Eq. (16), C is analogous to the momentum operator. In Eq. (16) we saw that C and B are canonically conjugate in a subspace which excludes the state $|\psi\rangle$ of Eq. (15). Thus, transforming arbitrary operators so that they annihilate the flat state is expected to be very useful, and we follow up on this idea below. We will refer to C and B as *generalized Weyl matrices* when the entries b_n are chosen arbitrarily.

We also mention work on a truncated harmonic oscillator restricted to operate in an N-dimensional Hilbert space [25–27] which leads to algebra similar to Eq. (14), but with fixed expressions for the matrices.

IV. THE ALGEBRA OF TYPE-1 MATRICES AND CONNECTION TO GENERALIZED WEYL MATRICES

A brief summary of type-1 matrix models is provided next; interested readers can find more details in the review in [9]. In [5–10], we developed a theory of sets of real symmetric $N \times N$ matrices depending linearly on a real parameter, say, x, as finite-dimensional prototypes of quantum integrable systems. They emerge from a study of the conservation laws of quantum integrable systems, such as one-dimensional (1D) Heisenberg and 1D Hubbard models, when they are restricted to finite sizes. The matrix formulation has the advantage of being "agnostic about" the originating quantum model while capturing elements related to their quantum integrability. Members of the commuting set are in the form $\alpha(x) = a + xA$, where a and A are $N \times N$ real symmetric matrices obeying certain constraint relations. A convenient formulation to define this set of matrices is to introduce N objects Z_j that play the role of a basis:

$$Z_j = |j\rangle\langle j| + x\sum_{k\neq j}\frac{1}{\epsilon_j - \epsilon_k}\big\{\, \gamma_j\gamma_k(|j\rangle\langle k| + |k\rangle\langle j|) - \gamma_j^2|k\rangle\langle k| - \gamma_k^2|j\rangle\langle j|\,\big\}, \tag{19}$$

where the commutation $[Z_j, Z_l] = 0$ for all j, l is established, with an unconstrained set of $2N + 1$ parameters $\{\gamma_j, \epsilon_j\}$ and x. We may then write $\alpha(x) = \sum_j c_j Z_j$, and varying the coefficients c_j generates the family of mutually commuting type-1 matrices.

In this program of constructing finite-dimensional matrices representing quantum integrable systems, we unexpectedly encountered an algebraic structure [10] that bears considerable resemblance to the problem in (14). We show here that our integrable matrix model and its conservation laws can be obtained purely from this algebra. This calculation thereby offers a different perspective on our model and provides further insights.

Our main cast consists of a set of matrix operators $\mathcal{S}$, $\mathcal{E}$, $\mathbf{\Gamma}$, and $\mathbf{D}$ with real entries acting on the N-dimensional real vector space $\mathcal{R}_N$. The antisymmetric matrix $\mathcal{S}$ is defined through its matrix elements

$$\mathcal{S}_{ij} = x\,(1 - \delta_{ij})\frac{\gamma_i\gamma_j}{\epsilon_i - \epsilon_j}, \quad \mathcal{S} = \sum_{i,j}|i\rangle\,\mathcal{S}_{ij}\,\langle j|, \tag{20}$$

where x is a real parameter, $\{\epsilon_1, \epsilon_2, \ldots, \epsilon_N\}$ are N real variables, and $\{\gamma_1, \gamma_2, \ldots, \gamma_N\}$ are N real numbers normalized by the condition

$$\sum_{i=1}^{N}\gamma_i^2 = 1. \tag{21}$$

We also need three diagonal matrices:

$$\mathcal{E} = \sum_{j=1}^{N}\epsilon_j|j\rangle\langle j|, \tag{22}$$

$$\mathbf{D} = \sum_{j=1}^{N}\gamma_j^2|j\rangle\langle j|, \tag{23}$$

and the projection operator

$$\mathbf{\Gamma} = |\gamma\rangle\langle\gamma|, \tag{24}$$

where

$$|\gamma\rangle = \sum_{j=1}^{N}\gamma_j|j\rangle. \tag{25}$$

It follows from the normalization of $\{\gamma_i\}$ that $\mathrm{Tr}\,\mathbf{\Gamma} = 1$ and $\mathrm{Tr}\,\mathbf{D} = 1$.

Comparing Eq. (20) with Eq. (12) shows that $\mathcal{S}$ is the same as C introduced earlier when the constants $\gamma_i \to 1$ and $\epsilon_i \to b_i$. With these changes, we see that $\mathcal{E}$ becomes B in Eq. (3) and $\mathbf{D}$ reduces to $\mathbb{1}$. Finally, we see that $\mathbf{\Gamma}$ is proportional to $|\psi\rangle\langle\psi|$, where $|\psi\rangle$ is given in Eq. (15), and the flat states $|\gamma\rangle$ map onto $|\psi\rangle$. With these changes, the algebra discussed below can be viewed as a generalization of Sec. III.

The commutator of $\mathcal{E}$ and $\mathcal{S}$ is easily seen to be

$$[\mathcal{E}, \mathcal{S}] = x\,(\mathbf{\Gamma} - \mathbf{D}), \tag{26}$$

with a vanishing trace of both sides, as expected. In the special case of $\gamma_i = \frac{1}{\sqrt{N}}$ for all i, we see that Eq. (26) reduces to Eq. (14) and x is analogous to Planck's constant.

Below we uncover N mutually commuting operators I_n [see Eq. (43)] using the three building blocks $\mathcal{E}$, $\mathbf{\Gamma}$, and $\mathcal{S}$. Among them, there is another natural candidate, Eq. (40), that can be viewed as the Hamiltonian. Indeed, we will see later that Eq. (40) is a natural Hamiltonian for a Grover-type quantum search algorithm, as discussed in [15–18].

A. A linear map of operators

Guided by our earlier discussion [see text below Eq. (18)], we now find a systematic method for mapping any operator to a related one which annihilates the projection operator $\mathbf{\Gamma}$. These operators are found by first analyzing the action of arbitrary operators $\mathcal{Q}$ on the state $|\gamma\rangle$. Guided by the form of Eq. (25), we now introduce a useful decomposition for any symmetric operator $\mathcal{Q}$:

$$\mathcal{Q} = \mathcal{Q}_{||} + \mathcal{Q}_{\perp}, \tag{27}$$

where $\mathcal{Q} = \sum_{ij} |i\rangle Q_{ij} \langle j|$ and $Q_{ij} = Q_{ji}$. The two pieces of $\mathcal{Q}$ have the property that

$$\mathcal{Q}|\gamma\rangle = \mathcal{Q}_{||}|\gamma\rangle, \quad \mathcal{Q}_{\perp}|\gamma\rangle = 0. \tag{28}$$

More explicitly,

$$\mathcal{Q}_{||} = \sum_{ij} |i\rangle\langle i|\, Q_{ij} \left(\frac{\gamma_j}{\gamma_i}\right) \tag{29}$$

and

$$\mathcal{Q}_{\perp} = -\frac{1}{2} \sum_{ij} \frac{1}{\gamma_i \gamma_j} \{|i\rangle\gamma_j - |j\rangle\gamma_i\}\, Q_{ij}\, \{\gamma_j \langle i| - \gamma_i \langle j|\}. \tag{30}$$

It is clear that $\mathcal{Q}_{\perp}$ annihilates the vector $|\gamma\rangle$ because the terms $\{\gamma_j\langle i| - \gamma_i\langle j|\}$ annihilate the state $|\gamma\rangle$ for every pair i, j. Using the symmetry of $\mathcal{Q}$, Eq. (30) also implies the orthogonality condition

$$\mathcal{Q}_{\perp} \cdot \mathbf{\Gamma} = 0 = \mathbf{\Gamma} \cdot \mathcal{Q}_{\perp}. \tag{31}$$

This construction can also be viewed as a linear map $\mathcal{Q} \to \mathcal{Q}_{||}$. To this end, we define the equal-amplitude (flat-sum) state $|\Phi\rangle$:

$$|\Phi\rangle = \sum_j |j\rangle. \tag{32}$$

It is useful to define an invertible diagonal operator

$$\tilde{\boldsymbol{\gamma}} = \sum_j \gamma_j |j\rangle\langle j|,$$
$$|\gamma\rangle = \tilde{\boldsymbol{\gamma}}|\Phi\rangle. \tag{33}$$

In terms of $\tilde{\boldsymbol{\gamma}}$ it is easy to see that

$$\mathcal{Q}_{||} \equiv \sum_j \langle j|\tilde{\boldsymbol{\gamma}}^{-1}\mathcal{Q}\tilde{\boldsymbol{\gamma}}|\Phi\rangle\, |j\rangle\langle j|. \tag{34}$$

In summary, the linear operator map (34) helps us to decompose an arbitrary real symmetric operator $\mathcal{Q}$ into two components, $\mathcal{Q} = \mathcal{Q}_{||} + \mathcal{Q}_{\perp}$, where the latter annihilates the state $|\gamma\rangle$.

B. Analogy with stochastic equations

A simple analogy between the construction in Eqs. (29), (30), and (34) and stochastic time-evolution equations in nonequilibrium physics may be helpful here. In the study of master equations, the equilibrium state can be used to perform a similarity transformation that enables the interpretation of the transition operator as a Hamiltonian and the master equation itself as the Euclidean version of Schrödinger's equation [28–30]. If we consider a state vector $|P\rangle$, with components representing the probabilities of the various basis states, and a transition operator $\mathcal{T}$ satisfying a master equation

$$\partial_t |P\rangle = -\mathcal{T}|P\rangle, \quad \langle\Phi|\mathcal{T} = 0, \tag{35}$$

where $|\Phi\rangle$ defined in Eq. (32) gives equal weight to every configuration $|i\rangle$, then the total probability is conserved. We can write the equilibrium state as

$$|P_{\rm eq}\rangle = \tilde{\boldsymbol{\gamma}}^2|\Phi\rangle = \sum_j \gamma_j^2 |j\rangle, \tag{36}$$

with positive weights for each configuration, so that the system flows to equilibrium provided $\mathcal{T}|P_{\rm eq}\rangle = 0$.

In order to transform this formulation to the Hamiltonian formulation we perform the similarity transformation

$$|P\rangle = \tilde{\boldsymbol{\gamma}}|\Psi\rangle, \quad H = \tilde{\boldsymbol{\gamma}}^{-1}\mathcal{T}\tilde{\boldsymbol{\gamma}}, \tag{37}$$

giving rise to the imaginary-time Schröedinger equation

$$\partial_t |\Psi\rangle = -H|\Psi\rangle. \tag{38}$$

The equilibrium distribution under this similarity transformation gives rise to the ground-state wave function $|\Psi_0\rangle \equiv \tilde{\boldsymbol{\gamma}}^{-1}|P_{\rm eq}\rangle = \tilde{\boldsymbol{\gamma}}|\Phi\rangle$, which satisfies the conditions

$$H|\Psi_0\rangle = 0 = \langle\Psi_0|H. \tag{39}$$

For a class of transition matrices this prescription gives a Hermitian Hamiltonian. The state $|\gamma\rangle$ in Eq. (33) now plays the role of the ground state $|\Psi_0\rangle$. This is the route taken in connecting Dyson's Brownian motion of matrices with the Calogero-Sutherland model of interacting particles in one dimension.

V. THE PARAMETER-DEPENDENT MATRIX HAMILTONIAN AND ITS CONSERVATION LAWS

Using the above algebra, we construct a Hamiltonian H as

$$H = \mathcal{E} + x(\mathbf{\Gamma} - \mathbb{1}) \equiv I_1. \tag{40}$$

We also refer to H as I_1 since, as we show below, it belongs to a family of matrices,

$$I_m = \mathcal{E}^m + [\mathcal{E}^m, \mathcal{S}]_{\perp}, \tag{41}$$

that commute among each other.

From Eq. (26) we note that the commutator $[\mathcal{E}^m, \mathcal{S}]$ is linear in x. We thus define

$$[\mathcal{E}^m, \mathcal{S}]_{\perp} \equiv x\, K_m, \tag{42}$$

so that the conservation laws (41) now read

$$I_m = \mathcal{E}^m + x\, K_m, \tag{43}$$

with $m = 1, 2, \ldots, N$. Here the effective Planck's constant x is arbitrary but common to all the members of this commuting family. Similar constants arise in most quantum integrable systems, e.g., the U parameter in the 1D Hubbard model. They satisfy, for all $n, m \leqslant N$,

$$[H, I_m] = 0, \tag{44}$$

$$[I_n, I_m] = 0. \tag{45}$$

In fact, we will begin by showing that the first member of the sequence in Eq. (43) is the Hamiltonian (40). For this purpose we use Eq. (26) to write

$$[\mathcal{E}, \mathcal{S}]_\perp = x(\mathbf{\Gamma} - \mathbf{D})_\perp = x(\mathbf{\Gamma} - \mathbb{1}), \tag{46}$$

where we used $\mathbf{D}_\perp = 0$, a result valid for any diagonal operator, thereby proving that $I_1 = H$. It may be useful to record the explicit form of the next conservation law,

$$I_2 = \mathcal{E}^2 + x(\mathcal{E}\mathbf{\Gamma} + \mathbf{\Gamma}\mathcal{E} - \mathcal{E} - \mathbb{1}\ \langle\gamma|\mathcal{E}|\gamma\rangle). \tag{47}$$

Let us now prove Eq. (44) for general m. The commutator is quadratic in x; hence, we need the vanishing of the three terms x^α, with $\alpha = 0, 1, 2$ separately. The constant term is trivial since $[\mathcal{E}, \mathcal{E}^m] = 0$. The $O(x)$ term requires

$$[\mathcal{E}^m, [\mathcal{E}, \mathcal{S}]_\perp] = [\mathcal{E}, [\mathcal{E}^m, \mathcal{S}]_\perp]. \tag{48}$$

We note that the perpendicularity condition can be dropped on both sides since the parallel part commutes with $\mathcal{E}$ and $\mathcal{E}^m$. We invoke the Jacobi identity

$$[\mathcal{E}^m, [\mathcal{E}, \mathcal{S}]] + [\mathcal{S}, [\mathcal{E}^m, \mathcal{E}]] + [\mathcal{E}, [\mathcal{S}, \mathcal{E}^m]] = 0, \tag{49}$$

and since the middle term is identically zero, this implies Eq. (48). The $O(x^2)$ term requires

$$\mathbf{\Gamma} \cdot [\mathcal{E}^m, \mathcal{S}]_\perp = [\mathcal{E}^m, \mathcal{S}]_\perp \cdot \mathbf{\Gamma}. \tag{50}$$

Now both sides vanish by the definition (31) of the orthogonality, and thereby we have proved Eq. (44) for any integer m.

A. Mutual commutation of I_n

If we assume that the spectrum of H is nondegenerate, the commutation of the operators (45) is implied by a standard argument from linear algebra. However, proving Eq. (45) directly without taking recourse to making assumptions about the spectrum of H is worthwhile. Note that we have proved Eq. (44) purely algebraically, without inquiring about the form of $\mathcal{S}$ and $\mathbf{D}$. It might be possible to do the same for Eq. (45), but we now present a proof that uses the explicit solution for $\mathcal{S}$ and $\mathbf{D}$.

Returning to Eq. (41) and using the explicit expressions (20), (22), and (23), we first work out

$$\frac{1}{x}\,[\mathcal{E}^m, S]_{ij} = \gamma_i\gamma_j \frac{\epsilon_i^m - \epsilon_j^m}{\epsilon_i - \epsilon_j}. \tag{51}$$

It is useful to introduce the vectors with circular brackets

$$|p) = \sum_j \gamma_j \epsilon_j^p |j\rangle, \tag{52}$$

so that $|0) = |\gamma\rangle$. We further define the overlap and projector $\mathcal{J}$,

$$(p|q) = \sigma_{p+q}, \quad \mathcal{J}(p, q) = |p)(q|, \tag{53}$$

where $\sigma_p = \sum \gamma_i^2 \epsilon_i^p$.

Thanks to the normalization, we have $\sigma_0 = 1$. In terms of these formulas we find

$$\frac{1}{x}\,[\mathcal{E}^m, S] = \sum_{r=0}^{m-1} \mathcal{J}(m-1-r, r) - m\sum_j \gamma_j^2 \epsilon_j^{m-1} |j\rangle\langle j|. \tag{54}$$

We can construct the perpendicular parts of these operators immediately from the definitions: In terms of a set of diagonal operators

$$\mathcal{E}^p = \sum_j \epsilon_j^p |j\rangle\langle j| \tag{55}$$

we obtain

$$\frac{1}{x}\,[\mathcal{E}^m, S]_\perp = K_m = \sum_{r=0}^{m-1} [\mathcal{J}(m-1-r, r) - \mathcal{E}^{m-1-r}\,\sigma_r], \tag{56}$$

so that

$$I_m = \mathcal{E}^m + x\sum_{r=0}^{m-1} [\mathcal{J}(m-1-r, r) - \mathcal{E}^{m-1-r}\,\sigma_r]. \tag{57}$$

With this explicit form for I_m, we compute the commutator

$$[I_m, I_n] = 0, \tag{58}$$

and the $O(x)$ term vanishes since we can ignore the $\perp$ constraint under the commutator with diagonal operators:

$$\begin{aligned}[\mathcal{E}^m, [\mathcal{E}^n, S]_\perp] - [\mathcal{E}^n, [\mathcal{E}^m, S]_\perp] \\ = [\mathcal{E}^m, [\mathcal{E}^n, S]] - [\mathcal{E}^n, [\mathcal{E}^m, S]].\end{aligned} \tag{59}$$

The right-hand side vanishes upon the application of the Jacobi identity. Thus, the only nontrivial condition to check is the $O(x^2)$ term $[K_m, K_n] = 0$, so we write

$$\begin{aligned}[K_m, K_n] &= \sum_{r=0}^{m-1}\sum_{s=0}^{n-1} [[\mathcal{J}(m-1-r, r) - \mathcal{E}^{m-1-r}\,\sigma_r], \\ &\quad \times [\mathcal{J}(n-1-s, s) - \mathcal{E}^{n-1-s}\,\sigma_s]], \\ &= \sum_{r=0}^{m-1}\sum_{s=0}^{n-1} [\sigma_\mu\,\bar{\mathcal{J}}(r, s) + \sigma_r\,\bar{\mathcal{J}}(s, \mu) + \sigma_s\,\bar{\mathcal{J}}(\mu, r)],\end{aligned} \tag{60}$$

where we abbreviated $\bar{\mathcal{J}}(a, b) = \mathcal{J}(a, b) - \mathcal{J}(b, a)$ and $\mu = m + n - 2 - r - s$ and used $\mathcal{E}^p|q) = |p + q)$. The term vanishes once the sum is performed, as we next show.

B. Proof of cancellation of Eq. (60)

Let us write $m \to m+1$ and $n \to n+1$ for convenience and write the $(-1\times)$ right-hand side of Eq. (60) in the form

$$\mathcal{Y} = \sum_{r=0}^{m}\sum_{s=0}^{n}\{s, r|m+n-r-s\}, \tag{61}$$

where we denote arbitrary integers by $a, b,$ and c and the symbol $\{\cdot\}$ stands for the cyclic sum,

$$\{a, b|c\} = [a, b; c] + [c, a; b] + [b, c; a],$$
$$[a, b; c] = \bar{\mathcal{J}}(a, b)\sigma_c. \tag{62}$$

In fact, the detailed form of $[a, b; c]$ is not important. The only property needed is the skew symmetry,

$$[a, b; c] = -[b, a; c]. \tag{63}$$

From these definitions it is easily seen that

$$\begin{aligned}
&\text{(i)}: \quad \{a, b|c\} = \{c, a|b\} = \{b, c|a\},\\
&\text{(ii)}: \quad \{a, b|c\} = -\{b, a|c\},\\
&\text{(iii)}: \quad \{a, a|c\} = 0.
\end{aligned} \tag{64}$$

We now separate $\mathcal{Y}$ into two parts assuming $m > n$,

$$\begin{aligned}
\mathcal{Y} &= \mathcal{Y}_1 + \mathcal{Y}_2,\\
\mathcal{Y}_1 &= \sum_{r=0}^{n}\sum_{s=0}^{n}\{s, r|m+n-r-s\},\\
\mathcal{Y}_2 &= \sum_{r=n+1}^{m}\sum_{s=0}^{n}\{s, r|m+n-r-s\}.
\end{aligned} \tag{65}$$

We first note that $\mathcal{Y}_1$ vanishes since the ranges of s and r are identical, so we can switch them, $r \leftrightarrow s$, and use property (ii) in Eq. (64), so that $\mathcal{Y}_1 = -\mathcal{Y}_1 = 0$. To analyze $\mathcal{Y}_2$, we fix r in its new range and observe that the resulting range of the integer $(m+n-r-s)$ coincides with that of s. For a given r we can now see that as s varies, there are two cases: (1) The integer $(m+n-r-s)$ equals s, which vanishes by using property (iii) in Eq. (64), or (2) the integer $(m+n-r-s)$ is distinct from s, in which case we can exchange them, $(m+n-r-s) \leftrightarrow s$, and then use property (ii) in Eq. (64) to show that the sum of these terms vanishes.

We have thus shown that the algebra (26) directly leads to the conservation laws I_n. We can take the linear sums $\sum_j c_j I_j$, and they are still constants of motion. The earlier construction of the type-1 family can be related to I_n straightforwardly. Indeed, we can express the operators I_m of Eq. (43) in terms of Z_j given by Eq. (19) as

$$I_n = \sum_j \epsilon_j^n Z_j. \tag{66}$$

Note that this relationship implies that only $N-1$ of the infinite sequence of I_n are linearly independent.

C. Spectra, recurrence relation, general formula, and I_n as a polynomial in H

The spectrum of a general type-1 matrix was determined in [6]. The eigenvalues ξ_α and unnormalized eigenvectors $|\varphi_\alpha\rangle$ (shared by all matrices in the commuting family) are

$$\xi_\alpha = x\sum_{i=1}^{N}\frac{d_i\gamma_i^2}{\lambda_\alpha - \epsilon_i}, \quad \varphi_\alpha^{(i)} = \frac{\gamma_i}{\lambda_\alpha - \epsilon_i}, \quad \alpha = 1, \ldots, N, \tag{67}$$

where d_i are the eigenvalues of the $x = 0$ part of the matrix and λ_α are the N roots of the equation

$$\sum_{i=1}^{N}\frac{\gamma_i^2}{\lambda_\alpha - \epsilon_i} = \frac{1}{x}. \tag{68}$$

For I_n we have $d_i = \epsilon_i^n$; i.e., the eigenvalues of I_n read

$$\eta_\alpha^{(n)} = x\sum_{i=1}^{N}\frac{\epsilon_i^n\gamma_i^2}{\lambda_\alpha - \epsilon_i}. \tag{69}$$

Note that when $x \to 0$, $\lambda_\alpha \to \epsilon_i$, and $\eta_\alpha^{(n)} \to \epsilon_i^n$. When $x \to \infty$, one λ_α (say, λ_N) diverges, while the others remain finite. Equation (68) implies

$$\lambda_N \to x\sum_i \gamma_i^2 = x. \tag{70}$$

The corresponding eigenvector (upon normalization) $|\varphi_N\rangle \to |\gamma\rangle$, and the eigenvalue $\eta_N^{(n)} \to 0$. Indeed, Eqs. (28) and (42) imply that $|\gamma\rangle$ is an eigenvector of I_n in the $x \to \infty$ limit with eigenvalue 0.

Eigenvalues of I_n are polynomials in λ_α of order n. Indeed, substituting the identity

$$\epsilon_i^n = (\epsilon_i - \lambda_\alpha)\big(\epsilon_i^{n-1} + \epsilon_i^{n-2}\lambda_\alpha + \cdots + \epsilon_i\lambda_\alpha^{n-1} + \lambda_\alpha^{n-1}\big) + \lambda_\alpha^n \tag{71}$$

into Eq. (69) and using Eq. (68), we derive

$$\eta_\alpha^{(n)} = \lambda_\alpha^n - x\sum_{k=1}^{n} a_k\lambda_\alpha^{n-k}, \quad a_k = \sum_{i=1}^{N}\epsilon_i^{k-1}\gamma_i^2 = \langle\gamma|\mathcal{E}^{k-1}|\gamma\rangle, \tag{72}$$

which also implies a recurrence relation for eigenvalues of I_n,

$$\eta_\alpha^{(n+1)} = \lambda_\alpha\eta_\alpha^{(n)} - xa_n. \tag{73}$$

Note in particular that the eigenvalues of H are

$$\eta_\alpha^{(1)} = \lambda_\alpha - x\sum_i \gamma_i^2 = \lambda_\alpha - x. \tag{74}$$

The above expressions for the eigenvalues are helpful in establishing several facts. For example, I_n is a polynomial in H of order n. To write down this polynomial, observe that the eigenvalues of $H + x\mathbb{1} = \mathcal{E} + x\boldsymbol{\Gamma}$ are simply λ_α, and Eqs. (72) and (73) therefore mean

$$\begin{aligned}
I_n &= (H + x\mathbb{1})^n - x\sum_{k=1}^{n}\langle\gamma|\mathcal{E}^{k-1}|\gamma\rangle(H + x\mathbb{1})^{n-k},\\
I_{n+1} &= HI_n + xI_n - x\langle\gamma|\mathcal{E}^n|\gamma\rangle.
\end{aligned} \tag{75}$$

Further, replacing $H + x\mathbb{1}$ with $\mathcal{E} + x\boldsymbol{\Gamma}$ in this equation and tracking down the terms linear in x (higher orders in x cancel

identically), we derive I_n explicitly in terms of $\mathcal{E}$ and $\mathbf{\Gamma}$,

$$\begin{aligned} I_n &= \mathcal{E}^n + xK_n \\ &= \mathcal{E}^n + x\sum_{k=1}^{n}(\mathcal{E}^{n-k}\mathbf{\Gamma}\mathcal{E}^{k-1} - \mathcal{E}^{n-k}\langle\gamma|\mathcal{E}^{k-1}|\gamma\rangle). \end{aligned} \tag{76}$$

Finally, let us obtain the eigenvalues $\kappa_\alpha^{(n)}$ of K_n. Evidently,

$$\kappa_\alpha^{(n)} = x^{-1}\lim_{x\to\infty}\eta_\alpha^{(n)}. \tag{77}$$

As discussed above, in this limit $\lambda_N \to x \to \infty$. Remaining $\lambda_\alpha \to \tilde{\lambda}_\alpha$, where $\tilde{\lambda}_\alpha$ are finite and are the roots of the equation

$$\sum_{i=1}^{N}\frac{\gamma_i^2}{\tilde{\lambda}_\alpha - \epsilon_i} = 0, \quad \alpha = 1,\ldots,N-1. \tag{78}$$

Plotting the left-hand side of this equation as a function of $\tilde{\lambda}_\alpha$, we observe that the roots are sandwiched between ϵ_i. Assuming ϵ_i are in ascending order, we have

$$\epsilon_1 < \tilde{\lambda}_1 < \epsilon_2 < \tilde{\lambda}_2 < \cdots < \epsilon_{N-1} < \tilde{\lambda}_{N-1} < \epsilon_N. \tag{79}$$

Further, Eq. (69) implies $\kappa_N^{(n)} = 0$ (these zero eigenvalues correspond to the common eigenvector $|\gamma\rangle$ of K_n), while Eq. (80) implies

$$\kappa_\alpha^{(n)} = -\sum_{k=1}^{n}\langle\gamma|\mathcal{E}^{k-1}|\gamma\rangle\tilde{\lambda}_\alpha^{m-k}, \quad \alpha = 1,\ldots,N-1. \tag{80}$$

Suppose all eigenvalues ϵ_i of $\mathcal{E}$ are non-negative and at least one of them is nonzero, i.e., $\mathcal{E}$ is a positive semidefinite matrix of nonzero rank. Then, Eqs. (79) and (80) imply that $\kappa_\alpha^{(n)} < 0$ for $\alpha = 1,\ldots,N-1$. It follows that $|\gamma\rangle$ is the ground state of $-K_n$ with eigenvalue 0.

VI. QUANTUM COMPUTATION WITH TYPE-1 MATRICES

We now explore the potential application of type-1 integrable matrices in quantum search algorithms. In the classical setting, locating a marked item in an unstructured database of size N requires, on average, $N/2$ queries. Grover's quantum algorithm [12,13] offers a quadratic speedup, reducing the query complexity to $O(\sqrt{N})$. We consider the adiabatic quantum computing implementation of this algorithm [15–18], in which the system evolves from a uniform superposition of all basis states to the target state under the specific time-dependent Hamiltonian $H_G(t)$ (referred to here as the Grover Hamiltonian). Remarkably, it turns out that $H_G(t)$ is type-1 matrix, namely, the Hamiltonian defined in Eq. (40). We next demonstrate how the commuting operators I_n can be exploited to enhance the fidelity of the quantum computation.

In quantum search algorithms [12–21], database items are represented as orthonormal basis states in Hilbert space. The computation begins in the uniform superposition [31]

$$|\gamma\rangle = \frac{1}{\sqrt{N}}\sum_{x=1}^{N}|x\rangle, \tag{81}$$

which equally weights all possible configurations. The goal is to identify a specific, unknown target state $|m\rangle$. Grover's algorithm achieves this by iteratively applying a sequence of unitary operations approximately $k \sim \pi\sqrt{N}/4$ times [12,13].

In contrast to this discrete-time protocol, we focus on an analog version of the quantum search [15–18]. The system evolves under the time-dependent Grover Hamiltonian

$$H_G(t) = s(t)[\mathbb{1} - |m\rangle\langle m|] + [1 - s(t)][\mathbb{1} - |\gamma\rangle\langle\gamma|], \tag{82}$$

with the interpolation function $s(t)$ satisfying $s(0) = 0$ and $s(T_{\text{run}}) = 1$. In a perfectly adiabatic evolution, the system would follow the instantaneous ground state from $|\gamma\rangle$ at $t = 0$ to the target state $|m\rangle$ at $t = T_{\text{run}}$. Achieving this ideal evolution would require an infinitely long run time, whereas the practical objective is to minimize T_{run} through a suitable choice of $s(t)$ while ensuring the final state remains sufficiently close to $|m\rangle$.

Roland and Cerf [18] showed that requiring the fidelity $F(t)$ between the evolving state $\Psi(t)$ and the instantaneous ground state $\Psi_0(t)$ to remain above a fixed threshold,

$$F(t) = |\langle\Psi_0(t)|\Psi(t)\rangle|^2 \geqslant F_{\min}, \tag{83}$$

throughout the evolution under the Hamiltonian (82)—that is, ensuring local adiabaticity—recovers the quadratic speedup of Grover's algorithm. Assuming $F_{\min}$ is close to 1 and applying the adiabatic theorem, they further derived the corresponding interpolation function $s(t)$ as

$$s(t) = \frac{N\tan\left(\frac{2t\delta}{N}\sqrt{N-1}\right)}{2\sqrt{N-1}\left[1+\sqrt{N-1}\tan\left(\frac{2t\delta}{N}\sqrt{N-1}\right)\right]}, \tag{84}$$

where $\delta = \sqrt{1 - F_{\min}}$. The complexity of this locally adiabatic evolution governed by $H_G(t)$ is then determined by the condition $s(T_{\text{run}}) = 1$, which yields

$$T_{\text{run}} = \frac{1}{\delta}\frac{N}{\sqrt{N-1}}\arctan\sqrt{N-1} \overset{N\gg 1}{\approx} \frac{\pi}{2\delta}\sqrt{N}. \tag{85}$$

We observe that the Grover Hamiltonian $H_G(t)$ is a special case of the type-1 Hamiltonian H. To see this, note that the Hamiltonian H defined in Eq. (40), along with its commuting partners I_n in Eq. (43), can be viewed as a two-parameter family of operators,

$$H = u\,\mathcal{E} + v\,(\mathbb{1} - \mathbf{\Gamma}), \quad I_n = u\,\mathcal{E}^n - v\,K_n, \tag{86}$$

where we have redefined $x = -v/u$ and rescaled all operators by an overall factor of u. This reparameterization leaves the commutation relations $[H, I_n] = [I_k, I_n] = 0$ unchanged. We now fix the basis in which $\mathcal{E}$ is diagonal so that $|1\rangle = |m\rangle$ and choose the parameters

$$\epsilon_1 = 0, \quad \epsilon_2 = \cdots = \epsilon_N = 1. \tag{87}$$

With this choice, $\mathcal{E} = \mathbb{1} - |m\rangle\langle m|$, and since $\mathbf{\Gamma} = |\gamma\rangle\langle\gamma|$ by definition, we find that $H = H_G(t)$ along the one-parameter trajectory $u = s(t)$ and $v = 1 - s(t)$ in the (u, v) parameter space. The fact that $H_G(t)$ lies within the type-1 family is notable, given that type-1 matrices form a measure-zero subset of all matrices of the form $M(u, v) = uA + vB$, where A and B are arbitrary real symmetric matrices independent of u and v [6,8].

As established in the previous section, when $\mathcal{E}$ is positive semidefinite with nonzero rank, all operators $-K_n$ have the same ground state $|\gamma\rangle$. Likewise, when $\epsilon_1 = 0$ and all other $\epsilon_i > 0$, the operators $\mathcal{E}^n$ have the common ground state $|1\rangle = |m\rangle$. It follows that the same adiabatic quantum computation

can be implemented using any of the commuting $I_n(t)$ as the interpolating Hamiltonian,

$$I_n(t) = s(t)\,\mathcal{E}^n + [1 - s(t)](-K_n). \tag{88}$$

This raises a natural question: How does the choice of $I_n(t)$ affect the accuracy of the computation? To address this, we compare the fidelities

$$F_n = |\langle m|\Psi_{(n)}(T_{\rm run})\rangle|^2 \tag{89}$$

by numerically evaluating $\Psi_{(n)}(t)$, the solution of the nonstationary Schrödinger equation $i\,\partial_t\Psi = I_n(t)\,\Psi$, with the initial condition $|\Psi(0)\rangle = |\gamma\rangle$. For simplicity, we use the same interpolating function $s(t)$ given by Eq. (84) for all $I_n(t)$.

With the choice of ϵ_i in Eq. (87), all operators I_n, including $I_1 \equiv H = H_G$, are block diagonal, consisting of a common 2×2 block and an $(N-2)\times(N-2)$ block proportional to the identity matrix. This 2×2 block governs the time evolution of the initial uniform superposition state $|\gamma\rangle$ under I_n, and hence, the fidelities F_n are identical for all n. To see this, note that

$$|\gamma\rangle = \frac{1}{\sqrt{N}}|1\rangle + \frac{\sqrt{N-1}}{\sqrt{N}}\,|\tilde{2}\rangle, \tag{90}$$

where $|\tilde{2}\rangle$ is a normalized state orthogonal to $|1\rangle = |m\rangle$. The Hamiltonian H_G in Eq. (82) is the identity matrix plus outer products of vectors $|1\rangle$ and $|\tilde{2}\rangle$ with themselves and with each other. In the basis where $|1\rangle$ and $|\tilde{2}\rangle$ are the first two basis vectors, H_G assumes the claimed block-diagonal form. Equation (75) implies that all I_n inherit this structure since raising $H + x\,\mathbb{1}$ to any integer power preserves it.

According to Eqs. (69) and (68), the eigenvalues $\eta_1^{(n)}$ and $\eta_2^{(n)}$ of the 2×2 block of I_n for the choice of ϵ_i in Eq. (87) and $\gamma_i = 1/\sqrt{N}$ are given by

$$\eta_{1,2}^{(n)} = x\frac{N-1}{N}\frac{1}{\lambda_{1,2}-1}, \tag{91}$$

where λ_1 and λ_2 are the roots of the quadratic equation

$$\frac{1}{N}\left(\frac{1}{\lambda} + \frac{N-1}{\lambda-1}\right) = \frac{1}{x}. \tag{92}$$

Since I_n commute, their 2×2 blocks must commute as well. Commuting 2×2 matrices with identical eigenvalues must coincide.

We now turn to other choices of positive-semidefinite $\mathcal{E}$ with $\epsilon_1 = 0$ and all other $\epsilon_i > 0$. As shown above, the same quantum search protocol can be implemented for any such $\mathcal{E}$ using any member I_n of the commuting type-1 family. Consider, for example, the following parameter choice:

$$\epsilon_1 = 0, \quad \epsilon_2 = 1, \tag{93}$$

and ϵ_i are uniformly distributed random numbers in the interval $[1.0, 1.0 + \Delta\epsilon]$ for $i > 2$ with $\Delta\epsilon$ being a small positive number. By construction, the energy gap between the ground and first excited states at $t = T_{\rm run}$ is the same (equal to 1) for all $I_n(t)$ and for the Grover Hamiltonian (82). In addition, this gap is also fixed at 1 for all $I_1(t) \equiv H(t)$ at $t = 0$, regardless of the specific choice of ϵ_i for $i > 2$. In this case, the Hamiltonian and the operators I_n are no longer block diagonal. Consequently, the instantaneous ground state is coupled not only to the first excited state but also to higher excited states, and the fidelities F_n become distinct. As shown in Fig. 1(a), the gap between the instantaneous ground state and the first excited state is nearly the same as that for the Grover Hamiltonian (82) across all I_n.

At first glance, one might expect that quantum tunneling to higher excited states would reduce the fidelity by increasing probability leakage out of the ground state. Surprisingly, our numerical simulations indicate the opposite behavior (see Fig. 1). The fidelity F_n exceeds that of the Grover Hamiltonian (82) for all I_n, and for $n = 3$, the fidelity deficit $1 - F_n$ is smaller by *2 orders of magnitude*. This enhancement is a result of quantum interference: Probability amplitudes for transitions out of the ground state combine destructively, suppressing leakage into excited states.

Figure 2 examines F_3 more closely for $n = 3$ and $N = 64$. In Fig. 2(a), two sets of random $\epsilon_{i>2}$ are drawn for various $\Delta\epsilon$, keeping $\delta = 0.1$ fixed. As $\Delta\epsilon \to 0$, the fidelity approaches that of the Grover Hamiltonian. In this instance, the best performance occurs for Random Choice #2 at $\Delta\epsilon = 0.1$. Figure 2(b) explores the effect of varying δ at fixed $\Delta\epsilon = 0.1$. As expected, lowering δ improves fidelity, at the cost of a longer $T_{\rm run}$.

Recall that the functional form of the interpolating schedule depends on two factors: (1) the energy gap $(\eta_2 - \eta_1)$ between the instantaneous ground state $\Psi_0(t)$ and the first excited state $\Psi_1(t)$ and (2) the transition matrix element $\langle\Psi_1(t)|dI_n(s)/ds|\Psi_0(t)\rangle = \langle\Psi_1(t)|(\mathcal{E}^n + K_n)|\Psi_0(t)\rangle$ [18]. In particular, the anneal-rate bound reads

$$\left|\frac{ds(t)}{dt}\right| \leqslant \delta\frac{(\eta_2-\eta_1)^2}{\left|\langle\Psi_1(t)|\frac{dI_n(s)}{ds}|\Psi_0(t)\rangle\right|}. \tag{94}$$

Using the Cauchy-Schwartz inequality, we obtain $\langle\Psi_1(t)|dI_n(s)/ds|\Psi_0(t)\rangle = O(1)$. Following the Grover case [18], we set $|\langle\Psi_1(t)|dI_n(s)/ds|\Psi_0(t)\rangle| = 1$ to (effectively) saturate the bound in Eq. (94). Our numerical results confirm the assertion *a posteriori*. Had the transition matrix element's magnitude substantially exceeded unity, achieving comparable fidelities F_n would have required a much slower anneal rate. Since $(\eta_2 - \eta_1)$ is approximately the same as for the Grover Hamiltonian (see Fig. 1), we use a single interpolating function for all $I_n(t)$. It follows that $T_{\rm run} \propto \sqrt{N}$ for every interpolating Hamiltonian, and the higher type-1 matrices deliver a constant-factor improvement over the Grover Hamiltonian.

It is worth noting that type-1 matrices also give rise to certain integrable multilevel Landau-Zener models [33,34]. These models are known to exhibit similarly favorable quantum interference effects among transition amplitudes [35–37]. These results indicate that exploiting the integrability of type-1 matrices within adiabatic quantum computation can meaningfully enhance performance. The commuting hierarchy supplies a systematic route to new interpolating Hamiltonians, furnishing an additional knob for tuning Grover-style search efficiency. It is also natural to ask whether controlled departures from integrability might yield further gains.

To conclude this section, we highlight several features relevant for physically implementing the analog Grover

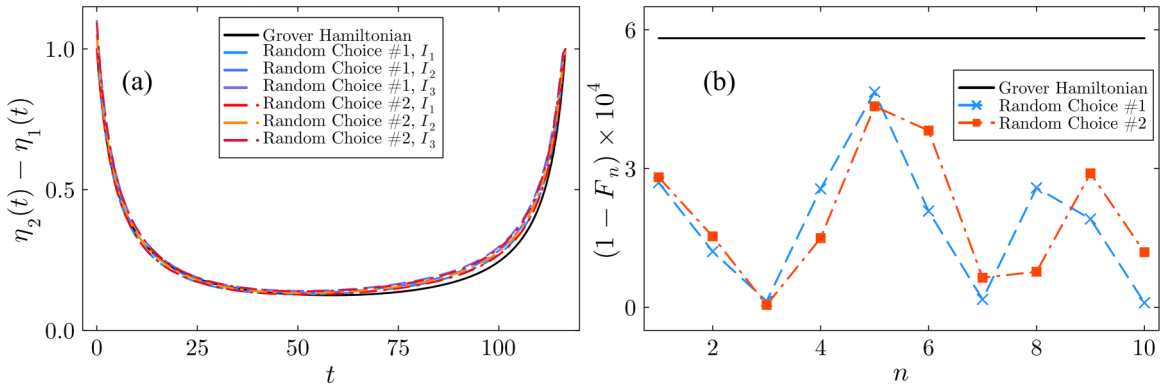

FIG. 1. Efficiency increase of Grover's search algorithm by utilizing quantum integrability of type-1 matrices. (a) Instantaneous energy gaps between the ground and first excited states as a function of $t \in (0, T_{\text{run}})$ for two random sets of $\epsilon_{i>2}$ with $\Delta\epsilon = 0.1$ and three different currents I_n as well as for the Grover Hamiltonian (solid black line). (b) $(1 - F_n)$ for different $I_n(t)$ and the same random sets of $\epsilon_{i>2}$ as in (a), where F_n is the fidelity. The increased fidelity compared to the Grover Hamiltonian (horizontal black line) is due to quantum interference. This effect is particularly dramatic for $n = 3$ and $n = 7$, with $1 - F_3 = 5.20 \times 10^{-6}$ and $1 - F_7 = 6.40 \times 10^{-5}$ for Random Choice #2 [32]. The matrix size is $N = 64$, and the parameter $\delta = 0.1$ in the interpolating function $s(t)$.

search using type-1 commuting partners. Realizing the Grover Hamiltonian for a database of size $N = 2^k$ with k qubits inevitably generates up to k-body interactions that are long-range under any geometry [16]. They include terms of the form $\prod_{i\in\mathbb{S}} \hat{\sigma}_{z_i}$ and $\prod_{i\in\mathbb{S}} \hat{\sigma}_{x_i}$, where $\hat{\sigma}_z$ and $\hat{\sigma}_x$ are Pauli operators and $\mathbb{S} \subseteq \{1, 2, \ldots, k\}$. One partial route toward physical realizability is provided by so-called gadget Hamiltonians, which replace such high-order interactions by enlarged Hamiltonians with only simple (typically two-body) couplings while reproducing the target Hamiltonian within a low-energy sector. Although gadgetized constructions [38–43] and several other proposed physical implementations of the Grover Hamiltonian [44,45] involve only two-body interactions, the resulting Hamiltonians remain intrinsically long range. These Hamiltonians are structurally analogous to Gaudin magnets, in which a distinguished degree of freedom couples collectively to the rest of the system [46]. In this light, we note that the commuting partners of the type-1 family, specifically the operators Z_j in Eq. (19), are themselves equivalent to Gaudin-type Hamiltonians [6]. This observation clarifies that extending the analog Grover protocol using higher integrals I_n does not introduce qualitatively new implementation challenges beyond those already present for the original Grover Hamiltonian. We therefore expect the mapping presented in Ref. [6] along with Eq. (66) to provide a practical route for realizing the full type-1 commuting hierarchy with comparable experimental overhead.

VII. CONCLUDING REMARKS

In this work, we noted that Weyl's relations involving two unitary matrices A and B in N dimensions can be usefully generalized to include a third matrix C. Matrix C has interesting commutation relations with $\ln A$, which permits one to view it as a finite-dimensional version of the operator $\hat{Q}\hat{P} + \hat{P}\hat{Q}$ in quantum mechanics, while its commutation relation with B enables one to view it as the canonical momentum $\hat{P}$ when it is restricted to an $(N - 1)$-dimensional subspace obtained through the elimination of a specific state of the original state space. A simple procedure for modifying arbitrary operators

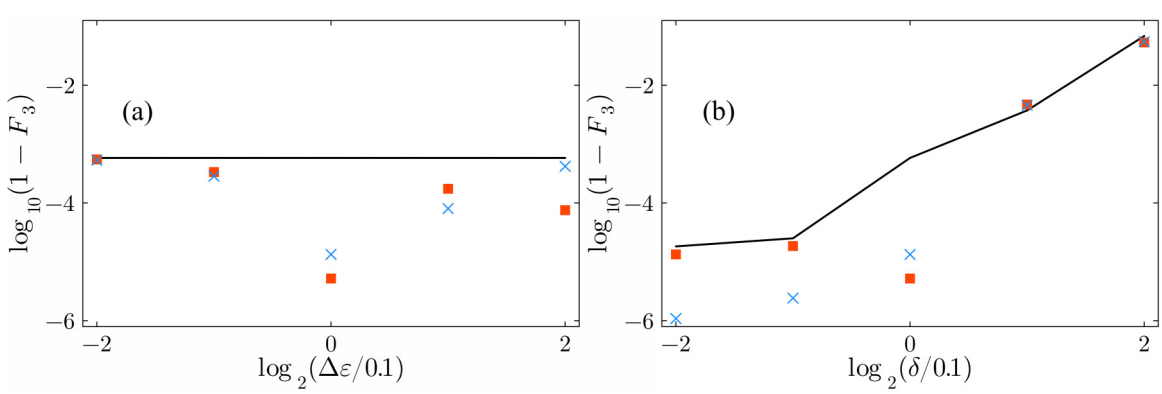

FIG. 2. Efficiency gain using I_3 for matrix size $N = 64$. (a) Five values of $\Delta\epsilon$, spaced logarithmically, are tested with fixed $\delta = 0.1$. Random Choices #1 and #2 are shown as blue crosses and red squares, respectively [32]. As $\Delta\epsilon \to 0$, the fidelity deficit converges to that of the Grover Hamiltonian (black line). Notably, the performance of I_3 improves markedly at $\Delta\epsilon = 0.1$. (b) Holding $\Delta\epsilon = 0.1$ fixed, we vary δ using the same random ϵ_i as in Fig. 1. As expected, both T_{run} and F_3 increase with decreasing δ. Curiously, lowering δ brings out a marked efficiency gain in Random Choice #1, driven by quantum integrability.

(matrices) to annihilate the specific state then generates an effectively finite-dimensional canonical theory. These matrices are then used to construct a hierarchy of mutually commuting operators, depending on $\sim 2N$ independent real parameters. These operators were shown to be intimately connected to type-1 matrices developed by us earlier [9] using very different and independently developed ideas. The type-1 matrices provide a realization of quantum integrable systems, such as the Heisenberg antiferromagnetic spin chain and the one-dimensional Hubbard model, so that the new hierarchy can be viewed in the same light.

Additionally, we found that the hierarchy of commuting operators obtained here contains the leading member I_1, given by Eq. (40), which, for a certain choice of the parameters, is identical to the Grover Hamiltonian (82) widely studied in the field of quantum computation. We presented results that suggest a significant advantage of employing higher members I_n with $n \geqslant 2$ in similar studies, which seem to be worth pursuing further.

Finally, we find it most remarkable that Weyl's ideas [1] continue to nourish current research and open new directions nearly a century after their original publication.

ACKNOWLEDGMENTS

We are grateful to D. Šafránek for bringing Ref. [18] to our attention. A.P. acknowledges the financial support from the Institute for Basic Science (IBS) in the Republic of Korea through Project No. IBS-R024-D1.

DATA AVAILABILITY

The data that support the findings of this article are not publicly available. The data are available from the authors upon reasonable request.

APPENDIX: DERIVING THE HEISENBERG ALGEBRA FROM THE WEYL MATRICES BY TAKING THE $N \to \infty$ LIMIT

In this appendix, we start with the pair of $N \times N$ unitary matrices A and B as introduced in Sec. III. We then lay out the derivation of the Heisenberg algebra in full.

Following Schwinger [3], we make a symmetric choice,

$$\xi = \eta = \sqrt{\omega_0}. \tag{A1}$$

We must also deal with the situation that the eigenvalues of $\ln B$, namely, $i\omega_0 n$, are discrete with a small spacing, while the eigenvalues of $\hat{Q} \to x$ are quasicontinuous; indeed, we would like to take the continuum limit to be $N \to \infty$. This is achieved by the Weyl scaling, where

$$x \leftrightarrow \sqrt{\omega_0}\, n, \quad |x\rangle \leftrightarrow \frac{1}{\sqrt[4]{\omega_0}}|n\rangle, \tag{A2}$$

so that the lattice constant $\sqrt{\omega_0}$ shrinks as N increases. With

$$x_1 = \sqrt{\omega_0}\, n, \quad x_2 = \sqrt{\omega_0}\, m, \tag{A3}$$

the Dirac delta overlap of the continuum states is related to the Kronecker delta overlap in the discrete case through the relation

$$\langle x_1|x_2\rangle = \delta(x_1 - x_2) \leftrightarrow \frac{1}{\sqrt{\omega_0}}\delta_{n,m}. \tag{A4}$$

A completely parallel situation exists for the momentum operator $\hat{P}$, which also has a continuous set of eigenvalues in the large-N-limit case. We skip its discussion since we need only Eqs. (A1) and (A4) below.

On the other hand, we now regard N as finite and compute the logarithms of the matrices and evaluate their commutators. We begin with

$$\ln B = i\omega_0 \sum_{n=0}^{N-1} n\, |n\rangle\langle n| \tag{A5}$$

and

$$\ln A = i\omega_0 \sum_{r=0}^{N-1} r|k_r\rangle\langle k_r|. \tag{A6}$$

Using Eq. (6), we obtain

$$\begin{aligned}\ln A &= i\pi\left(1 - \frac{1}{N}\right)\mathbb{1} + i\frac{\pi}{N}\sum_{n\neq m} \\ &\quad \times \frac{|n\rangle\langle m|b_m - |m\rangle\langle n|b_n}{b_n - b_m}, \end{aligned} \tag{A7}$$

$$\begin{aligned}&= i\pi\left(1 - \frac{1}{N}\right)\mathbb{1} + i\frac{\pi}{N}\sum_{n\neq m} \\ &\quad \times \left[\cot\frac{\pi}{N}(n-m) - i\right]|n\rangle\langle m|, \end{aligned} \tag{A8}$$

with the second form (A8) illustrating the useful result that convolution with the cotangent in real space is equivalent to the first derivative for a class of functions on the lattice [47].

Going further, we compute the matrix element of the commutator [48]. Denoting $\Delta = \omega_0(n - m)$ and treating Δ formally as a continuous variable, we obtain the matrix element

$$\begin{aligned}\langle n|\,[\ln B, \ln A]\,|m\rangle &= -\frac{\omega_0}{N}\Delta\sum_{r=0}^{N-1} r e^{i\Delta r} \\ &= i\frac{\omega_0}{N}\Delta\frac{d}{d\Delta}\left(e^{i\frac{1}{2}\Delta(N-1)}\frac{\sin\frac{1}{2}\Delta N}{\sin\frac{1}{2}\Delta}\right). \end{aligned} \tag{A9}$$

Further, Eq. (A3) implies $\Delta = \sqrt{\omega_0}(x_1 - x_2)$, and using Eq. (A1), we rewrite Eq. (A9) as

$$\begin{aligned}&\sqrt{\omega_0}\langle x_1|[\ln B, \ln A]|x_2\rangle \\ &\quad = i\frac{\omega_0}{N}(x_1 - x_2)\frac{d}{d(x_1 - x_2)} \\ &\quad \times \left(e^{ic_0(x_1 - x_2)}\frac{\sin\sqrt{\frac{1}{2}\pi N}(x_1 - x_2)}{\sin\sqrt{\frac{\pi}{2N}}(x_1 - x_2)}\right), \end{aligned} \tag{A10}$$

where $c_0 = \frac{1}{2}\sqrt{\omega_0}(N-1)$. By using the Dirichlet-Bonnet result [49], we can set

$$\lim_{N\to\infty} \frac{\sin\sqrt{\frac{1}{2}\pi N}(x_1 - x_2)}{\sin\sqrt{\frac{\pi}{2N}}(x_1 - x_2)} \to \frac{2\pi}{\sqrt{\omega_0}}\delta(x_1 - x_2). \quad \text{(A11)}$$

If we use $(x_1 - x_2)\delta'(x_1 - x_2) = -\delta(x_1 - x_2)$, Eq. (A10) reduces to

$$\sqrt{\omega_0}\langle x_1|[\ln B, \ln A]|x_2\rangle = -i(\omega_0)^{\frac{3}{2}}\delta(x_1 - x_2). \quad \text{(A12)}$$

Using the replacements $\ln B \to i\sqrt{\omega_0}\hat{Q}$ and $\ln A \to i\sqrt{\omega_0}\hat{P}/\hbar$ and canceling the common $\omega_0^{\frac{3}{2}}$ term, we recover the matrix elements of the Heisenberg algebra (1),

$$\langle x_1|[\hat{Q}, \hat{P}]|x_2\rangle = i\hbar\delta(x_1 - x_2). \quad \text{(A13)}$$

[1] H. Weyl, Quantenmechanik und Gruppentheorie, Z. Phys. **46**, 1 (1927); *Theory of Groups and Quantum Mechanics* (Dover, New York, 1950).

[2] J. Schwinger, Unitary operator bases, Proc. Natl. Acad. Sci. USA **46**, 570 (1960).

[3] J. Schwinger, The special canonical group, Proc. Natl. Acad. Sci. USA **46**, 1401 (1960).

[4] T. S. Santhanam and A. R. Tekumalla, Quantum mechanics in finite dimensions, Found. Phys. **6**, 583 (1976).

[5] B. S. Shastry, A class of parameter-dependent commuting matrices, J. Phys. A **38**, L431 (2005).

[6] H. K. Owusu, K. Wagh, and E. A. Yuzbashyan, The link between integrability, level crossings, and exact solution in quantum models, J. Phys. A **42**, 035206 (2009).

[7] B. S. Shastry, Parameter dependent commuting matrices, Plücker relations and related quantum glass models, J. Phys. A **44**, 052001 (2011).

[8] H. K. Owusu and E. A. Yuzbashyan, Classification of parameter-dependent quantum integrable models, their parameterization, exact solution and other properties, J. Phys. A **44**, 395302 (2011).

[9] E. A. Yuzbashyan and B. S. Shastry, Quantum integrability in systems with finite number of levels, J. Stat. Phys. **150**, 704 (2013).

[10] E. A. Yuzbashyan, B. S. Shastry, and J. A. Scaramazza, Rotationally invariant ensembles of integrable matrices, Phys. Rev. E **93**, 052114 (2016).

[11] J. A. Scaramazza, B. S. Shastry, and E. A. Yuzbashyan, Integrable matrix theory: Level statistics, Phys. Rev. E **94**, 032106 (2016).

[12] L. K. Grover, A fast quantum mechanical algorithm for database search, in *STOC '96: Proceedings of the Twenty-Eighth Annual ACM Symposium on Theory of Computing* (Association for Computing Machinery, New York, 1996), pp. 212–219.

[13] L. K. Grover, Quantum mechanics helps in searching for a needle in a haystack, Phys. Rev. Lett. **79**, 325 (1997).

[14] M. Boyer, G. Brassard, P. Høyer, and A. Tapp, Tight bounds on quantum searching, Fortschr. Phys. **46**, 493 (1998).

[15] E. Farhi and S. Gutmann, Analog of a digital quantum computation, Phys. Rev. A **57**, 2403 (1998).

[16] E. Farhi, J. Goldstone, S. Gutmann, and M. Sipser, Quantum computation by adiabatic evolution, arXiv:quant-ph/0001106.

[17] E. Farhi, J. Goldstone, S. Gutmann, J. Lapan, A. Lundgren, and D. Preda, A quantum adiabatic evolution algorithm applied to random instances of an NP-complete problem, Science **292**, 472 (2001).

[18] J. Roland and N. J. Cerf, Quantum search by local adiabatic evolution, Phys. Rev. A **65**, 042308 (2002).

[19] B. W. Reichardt, The quantum adiabatic optimization algorithm and local minima, in *STOC '04: Proceedings of the Thirty-Sixth Annual ACM Symposium on Theory of Computing* (Association for Computing Machinery, New York, 2004), pp. 502–510.

[20] A. M. Childs and J. Goldstone, Spatial search by quantum walk, Phys. Rev. A **70**, 022314 (2004).

[21] A. P. Young, S. Knysh, and V. N. Smelyanskiy, First-order phase transition in the quantum adiabatic algorithm, Phys. Rev. Lett. **104**, 020502 (2010).

[22] Weyl [1] notes, "The commutation rules which are satisfied by q, p in quantum mechanics cause some trouble" (p. 255). He outlines a general procedure for taking the continuum limit to obtain the Heisenberg commutation relations "symbolically" written as $q(x)p(x') - p(x')q(x) = i\delta(x - x')$ (see Eq. (12.3) in [1]), with the notation $\delta(x - x') = \frac{1}{\Delta x}\delta_{xx'}$ (p. 254), and $\Delta x = \frac{1}{N}$, with $\Delta x \to 0$ in the limit of large N. In the present case it is appropriate to take $\Delta x = \frac{\sqrt{2\pi}}{\sqrt{N}}$, leading to Eqs. (A2) and (A4). With this choice of Δx, also vanishing in the large-N limit, the matrix element equation (A13) leads systematically to the Heisenberg commutator (1), as shown. We call this refined procedure Weyl's scaling.

[23] C. H. Bennett, G. Brassard, C. Crepeau, R. Jozsa, A. Peres, and W. K. Wootters, Teleporting an unknown quantum state via dual classical and Einstein-Podolsky-Rosen channels, Phys. Rev. Lett. **70**, 1895 (1993).

[24] R. A. Bertlmann and P. Krammer, Entanglement witnesses and geometry of entanglement of two-qutrit states, Ann. Phys. (Amsterdam, Neth.) **324**, 1388 (2009).

[25] B. Baumgartner, B. Hiesmayr, and H. Narnhofer, A special simplex in the state space for entangled qudits, J. Phys. A **40**, 7919 (2007).

[26] H. A. Buchdahl, Concerning a kind of truncated quantized linear harmonic oscillator, Am J. Phys. **35**, 210 (1967).

[27] S. L. Trubatch, Generalized finite matrix Hamiltonians, Am J. Phys. **39**, 327 (1971).

[28] B. Bagchi and P. K. Roy, A new look at the harmonic oscillator problem in a finite-dimensional Hilbert space, Phys. Lett. A **200**, 411 (1995).

[29] K. Kawasaki, Diffusion constants near the critical point for time-dependent Ising models. I, Phys. Rev. **145**, 224 (1966).

[30] L. P. Kadanoff and J. Swift, Transport coefficients near the liquid-gas critical point, Phys. Rev. **165**, 310 (1968).

[31] E. D. Siggia, Pseudospin formulation of kinetic Ising models, Phys. Rev. B **16**, 2319 (1977).

[32] Here we have anticipated the connection between the uniform superposition and the projection operator $\mathbf{\Gamma}$, which is defined via state $|\gamma\rangle$ as $\mathbf{\Gamma} = |\gamma\rangle\langle\gamma|$.

[33] In the programming language julia, which we used to generate the figures, fixing $\Delta\epsilon$ and an integer seed determines a specific set of random values for $\epsilon_{i>2}$. We refer to seed values 1 and 2 as "Random Choice #1" and "Random Choice #2," respectively.

[34] A. Patra and E. A. Yuzbashyan, Quantum integrability in the multistate Landau–Zener problem, J. Phys. A **48**, 245303 (2015).

[35] E. A. Yuzbashyan, Integrable time-dependent Hamiltonians, solvable Landau–Zener models and Gaudin magnets, Ann. Phys. (Amsterdam, Neth.) **392**, 323 (2018).

[36] Yu. N. Demkov and V. N. Ostrovsky, Multipath interference in a multistate Landau-Zener-type model, Phys. Rev. A **61**, 032705 (2000).

[37] N. A. Sinitsyn, Exact transition probabilities in a 6-state Landau–Zener system with path interference, J. Phys. A **48**, 195305 (2015).

[38] N. A. Sinitsyn and V. Y. Chernyak, The quest for solvable multistate Landau-Zener models, J. Phys. A **50**, 255203 (2017).

[39] J. Kempe, A. Kitaev, and O. Regev, The complexity of the local Hamiltonian problem, SIAM J. Comput. **35**, 1070 (2006).

[40] N. Dattani, *Quadratization in Discrete Optimization and Quantum Mechanics* (Springer, Cham, 2019).

[41] S. P. Jordan and E. Farhi, Perturbative gadgets at arbitrary orders, Phys. Rev. A **77**, 062329 (2008).

[42] N. Chancellor, S. Zohren, P. A. Warburton, S. Benjamin, and S. Roberts, A direct mapping of Max k-SAT and high order parity checks to a Chimera graph, Sci. Rep. **6**, 37107 (2016).

[43] N. Chancellor, S. Zohren, and P. A. Warburton, Circuit design for multi-body interactions in superconducting quantum annealing systems with applications to a scalable architecture, npj Quantum Inf. **3**, 21 (2017).

[44] A. B. Dodds, V. Kendon, C. S. Adams, and N. Chancellor, Practical designs for permutation-symmetric problem Hamiltonians on hypercubes, Phys. Rev. A **100**, 032320 (2019).

[45] D. Daems and S. Guérin, Adiabatic quantum search scheme with atoms in a cavity driven by lasers, Phys. Rev. Lett. **99**, 170503 (2007).

[46] V. Pouthier, Exciton-mediated quantum search on a star graph, Quantum Inf. Process. **14**, 3139 (2015).

[47] M. Gaudin, Diagonalisation d'une classe d'hamiltoniens de spin, Note CEA **1559**, 1 (1972); J. Phys. (Paris) **37**, 1087 (1976); *La fonction d'onde de Bethe* (Masson, Paris, 1983).

[48] B. S. Shastry, Taking the square root of the discrete $1/r^2$ model, Phys. Rev. Lett. **69**, 164 (1992).

[49] E. T. Whittaker and G. N. Watson, *A Course of Modern Analysis*, 4th ed. (Cambridge University Press, Cambridge, 1969), Sec. 9.43, p. 176.